# The use of vectors for defining the three-dimensional texture and asymmetric directionality of turned specimens

**J Burrows**[1]*, **B Griffiths**[2] and **P Scott**[3]
[1]School of Manufacturing and Mechanical Engineering, University of Birmingham, UK
[2]Manufacturing and Engineering Systems Department, Brunel University, Uxbridge, Middlesex, UK
[3]Taylor Hobson Limited, Leicester, UK

**Abstract:** The authors consider that existing two-dimensional surface parameters (calculated using stylus profilometry techniques) are inadequate for describing engineering surfaces when the three-dimensional nature of an engineering surface also affects the functional performance. This paper proposes a definition of three-dimensional surface texture in terms of lay, directionality and anisotropy. The authors propose a novel technique developed from image processing technology, which uses vectors, to describe these three-dimensional surface properties. The proposed technique is validated via analysis of a series of turned surfaces.

**Keywords:** three-dimensional surface analysis, vectors, lay, directionality

## NOTATION

| | |
|---|---|
| AACF | areal autocorrelation function |
| $g_1$ | horizontal planar gradient function |
| $g_2$ | vertical planar gradient function |
| $G_x$ | horizontal planar gradient component |
| $G_y$ | vertical planar gradient component |
| $G_{(x,y)}$ | local gradient |
| $h_1, h_2$ | $3 \times 3$ operator matrices |
| $R_a$ | average roughness deviation from the mean |
| $R_q$ | root mean square of roughness deviation from the mean |
| $S_{al}$ | areal fastest decay autocorrelation function |
| $S_q$ | areal average roughness deviation from the mean |
| $S_{td}$ | areal texture direction |
| $S_{tr}$ | areal texture aspect ratio |
| $TnN$ | generic form of two-dimensional parameters |
| $z$ | equation of the plane |
| $\alpha$ | lay angle parallel to the surface plane |
| $\alpha(x, y)$ | local direction |
| $\beta$ | directionality angle orthogonal to the surface plane |
| $\theta$ | planar angle |

*The MS was received on 6 December 1999 and was accepted after revision for publication on 6 June 2000.*
**Corresponding author: School of Manufacturing and Mechanical Engineering, University of Birmingham, Room G47A, Edgbaston, Birmingham B15 2TT, UK.*

## 1 INTRODUCTION

Surface finish has been shown to influence functional performance in a large number of engineering situations [**1**, **2**], and therefore the surface finish produced by manufacturing processes is extremely important. Engineering surfaces are commonly inspected using profilometry in which a stylus is drawn across a surface producing an $x$–$z$ dataset. From this dataset, various two-dimensional parameters can be calculated which take the generic form $TnN$ [**3**]. Here, $T$ refers to the scale of measurement (e.g. roughness, $R$, or waviness, $W$), $n$ refers to the sample number (e.g. 1 to 5) and $N$ refers to the parameter calculated, e.g. $q$ for the root mean squared roughness or $sm$ for the peak mean spacing. These are all defined by international standards (BS 1134, ISO 4287: 1997). However, there is much evidence to show that the three-dimensional nature of surfaces also influences functional performance [**4**], as illustrated in Fig. 1. Figure 1 shows that either the lay, the directionality, the texture or the anisotropy influences a variety of functional performance situations. It has been assembled from general publications as well as the authors' research work. The survey represented by Fig. 1 shows that the three-dimensional nature of the surface influences functional performance. However, as yet there are no three-dimensional parameters defined by international standards that can be used to specify the three-dimensional characteristics of the performance situations represented by Fig. 1.

| | | Function | Heights | Distribution & Shape | Slopes & Curvature | Lengths & Peak | Lay & Lead |
|---|---|---|---|---|---|---|---|
| FUNCTIONAL RELATIONSHIPS | | Bearings | ● | ● | ◗ | ◗ | ● |
| | | Seals | ● | ● | ● | ◗ | ● |
| | | Friction | ● | ● | ● | ● | ● |
| | | Joint stiffness | ● | ● | ◗ | ◗ | ◗ |
| | | Slideways | ● | ● | ◗ | ● | ● |
| | | Contacts (elec/therm) | ● | ● | ● | ● | ? |
| | | Wear | ● | ● | ● | ● | ● |
| | | Galling | ● | ◗ | ● | ○ | ? |
| | | Adhesion & bonding | ● | ● | ◗ | ◗ | ◗ |
| | | Plating & painting | ● | ◗ | ◗ | ◗ | ? |
| | | Forming & drawing | ● | ◗ | ◗ | ● | ◗ |
| | | Fatigue | ● | ◗ | ○ | ○ | ● |
| | | Stress & fracture | ● | ○ | ◗ | ? | ● |
| | | Reflectivity | ● | ? | ● | ● | ● |
| | | Hygiene | ● | ◗ | ◗ | ? | ? |
| ASSESSMENT BY | STYLUS | Typical 2-D Parameters | Ra, Rq, Rt | Rsk, Rku, BAC | Da,Dq, Peak Curvature | La, Lq, Pc Correlation length | None |
| | | Typical 3-D Parameters | Sa, Sq | Ssk, Sku, Ssc | Sda, Ssc | Sal, Sdr | Std, Svi |
| | LIGHT | Typical Specular (1D) Parameters | Peak Intensity | None | None | None | None |
| | | Typical Diffuse (1D) Parameters | Angular Intensity | None | None | None | None |
| | | Typical 2-D Distribution Parameters | Peak/Total Intensity | None | Peak Shift Std. Dev. | Intensity Peaks | None |
| | | Typical 3-D blob Parameters | Peak Intensity Volume | None | Peak Shift Intensity | Intensity Peaks Blob Form | Cross Section |

Key: ● - Much Evidence, ◗ - Some Evidence, ○ - Little or Circumstantial Evidence, ?-Unknown

**Fig. 1** Relationships between surface parameters and engineering surface performance

This paper presents a method for describing the three-dimensional nature of surfaces using vectors, which provides a means of representing lay, directionality and anisotropy. The method is evaluated during analysis of a turned specimen.

## 2 SHORTCOMINGS OF TWO-DIMENSIONAL SURFACE MEASUREMENT

The single trace across a surface only provides information of the heights along that line. In many instances this

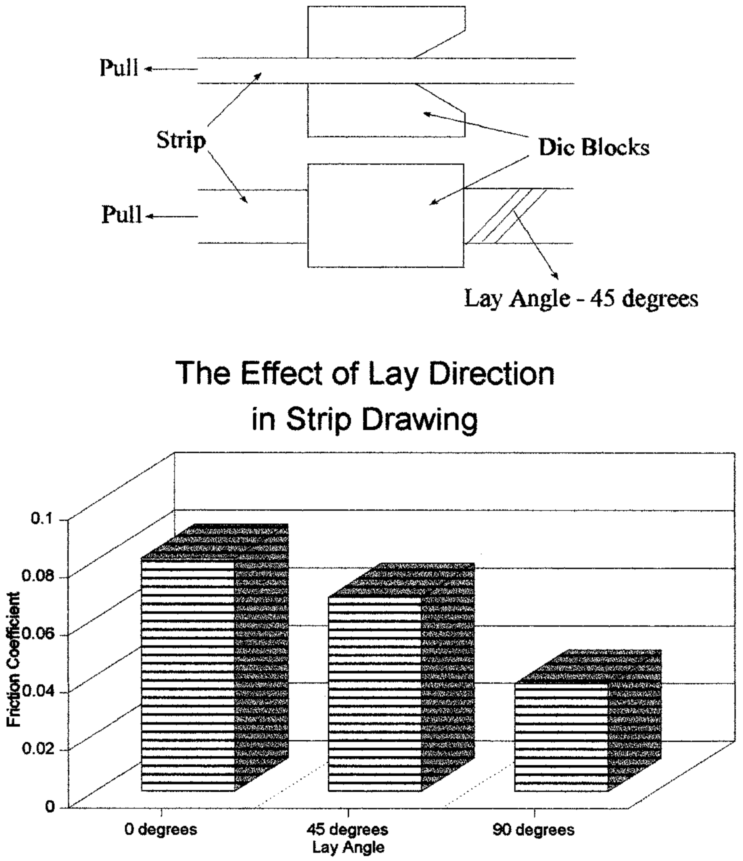


**Fig. 2** Effect of lay angle upon the coefficient of strip drawing friction

is entirely satisfactory. If the surface is anisotropic, like a ploughed field, then the worse case is produced by tracing across the lay, and often the worst case is what is wanted. However, the direction of importance is the functional one which is not necessarily across the lay. For example, in sheet metal drawing, the direction of the sheet surface lay could be in a variety of directions with respect to the die mouth. This is illustrated by the following experiment. A specially designed rig was used to draw steel strip [**5**]. The dies were flat and parallel. A series of steel strips with different textures were drawn. The strips were produced under identical abrasion conditions so that the surface finish was the same. The only difference between the strips was the angle of the abrasion direction with respect to the die mouth. Three angles were used and, as Fig. 2 shows, the die mouth friction was very different for each of the three samples, even though the surface finish was the same. When the texture direction is perpendicular to the die mouth, lubricant is captured, whereas when the texture is longitudinal to the die mouth and parallel with the pull drawing direction, lubricant is ejected. In the former case the captured lubricant gives low friction, whereas in the latter case the reduced lubrication gives high friction. If a two-dimensional stylus trace is taken in the direction of drawing, the measured surface finish is different, as peak spacing, and therefore roughness, change with the texture angle. When these surface finish values are related to the friction coefficient, it appears that, as either the roughness decreases or the peak spacing increases, the friction reduces. However, this is incorrect because the friction is related to the three-dimensional lay, texture and directionality and not the two-dimensional roughness. This fact is the basis for many of the examples shown in Fig. 1. Hence, there is a need to specify surfaces by three-dimensional roughness parameters so that the $T$ refers to an area rather than a line.

## 3 THREE-DIMENSIONAL SURFACE ASSESSMENT

In order to discuss three-dimensional surfaces, a schematic diagram is presented in Fig. 3. This defines the subsequent terminology used throughout the discussion below; namely, lay, directionality and connectivity.

To fulfil the requirements of industry and academia for three-dimensional surface description, numerous approaches have been researched in the literature, and are discussed below. In order to facilitate a direct comparison of these approaches, they are collated in

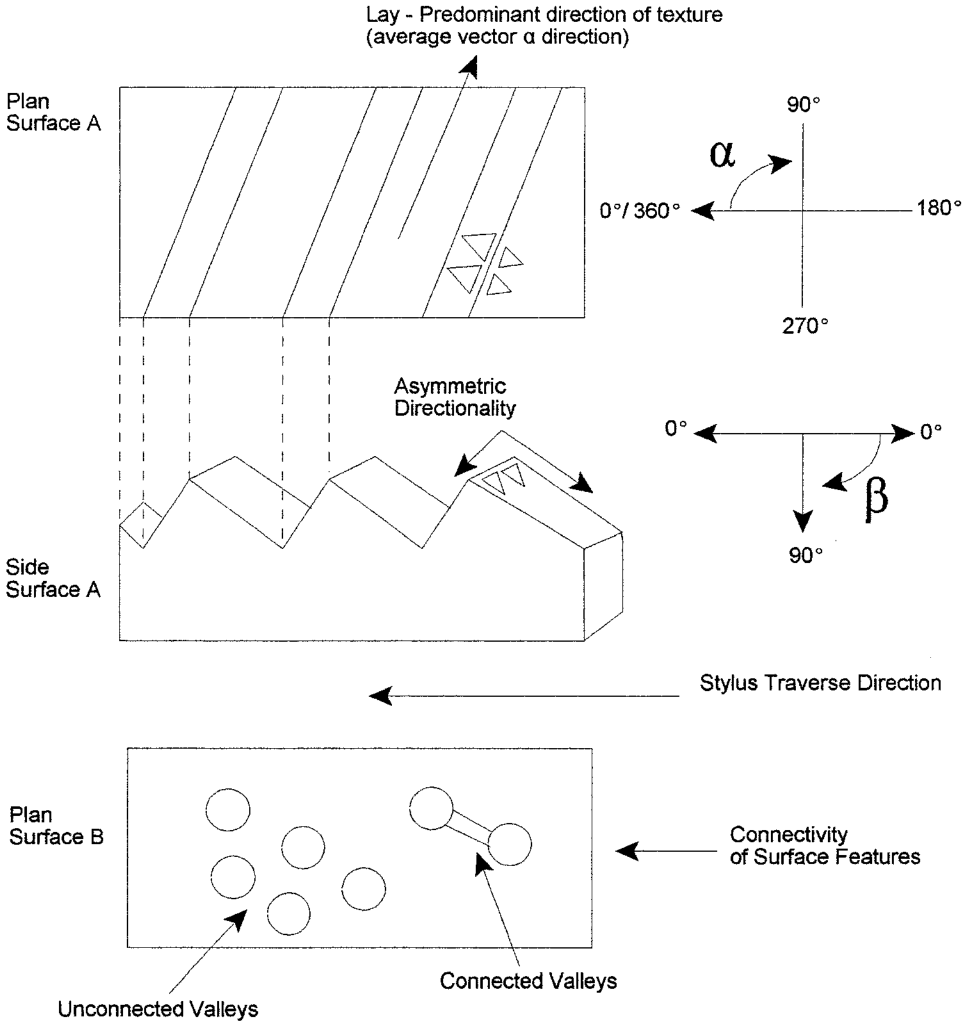


**Fig. 3** Schematic diagram of two surfaces denoting three-dimensional lay, directionality and connectivity

Table 1 under the following technique subdivisions: fractal analysis, statistical analysis, areal motifs and image processing. Table 1 proposes an appraisal of the methodologies compared with the three-dimensional primary parameter set as proposed by Dong *et al.* [**6**], using this proposal as the benchmark for discussion of the techniques. To assist this task, Table 1 assesses each of the major classes of technique with respect to two criteria: the ability of the technique to replicate and/or produce results as proposed in the three-dimensional primary parameter set and the ability of the technique to define functional performance characteristics of surfaces, including lay, directionality and connectivity.

At present there are no three-dimensional surface roughness parameters defined in the international standards, although some recommendations have been made. The report of an EU grant on surface characteri-

**Table 1** Proposed three-dimensional surface representation techniques, detailing their ability to reproduce to the proposed three-dimensional parameters and describe three-dimensional surface properties [**12**]

| | | 3D proposed parameters | | | 3D surface properties | | |
|---|---|---|---|---|---|---|---|
| Author | Technique | Heights | Spatial | Hybrid | Lay | Directionality | Connectivity |
| Dong *et al.* (1994) | Proposed 3D parameters | ✓ | ✓ | ✓ | ✓ | × | × |
| Zahouani/Barre (1997) | Spectral rose | × | × | × | ✓ | × | × |
| Scott (1997) | Areal motif | ✓ | ✓ | ? | ? | × | ✓ |
| Pfestorf *et al.* (1997) | Areal volume | ✓ | ? | ? | ? | × | ✓ |
| Russ/Brown (1997) | Fractals | × | × | × | ? | × | ? |
| Kovalyov and Chizhik (1993) | Image processing | × | ? | × | ✓ | × | × |

zation recommends the adoption of $S$ for areal surface roughness parameters [7]. The EU report went further in that it recommended a primary set of 14 parameters. For convenience, these can be divided into two sets:

(a) three-dimensional versions of traditional two-dimensional parameters, e.g. $S_q$ being the areal r.m.s. value which in two dimensions is $R_q$;
(b) new parameters that define some aspect of the three-dimensional dataset.

With respect to anisotropy, there are three parameters of interest:

(a) the texture direction $S_{td}$,
(b) the texture aspect ratio $S_{tr}$,
(c) the fastest decay autocorrelation length $S_{al}$.

Each of these three parameters is defined in the report mentioned previously [7]. With reference to Fig. 2, the use of $S_{td}$, $S_{tr}$ and $S_{al}$ may be used to determine the lay angle of the strip. However, it would not be possible to use any of these parameters to calculate the directionality of the strip and therefore any anisotropy of the surface. Alternative methods for defining the texture directionality have been based on Rose diagrams which can be derived from either the angular distribution [8], the contour lines or the structure function [9].

All these provide directly or indirectly the dominant surface texture angle which is obviously useful in cases such as the sheet drawing example above. However, the disadvantage of these techniques [7–9] is that they are unable to provide directionality information, and the directionality of a surface may greatly affect its functional performance. For instance, an anisometric surface (as produced by a turning tool ground with a plan approach angle that is different from the plan trail angle) would have different functional performance characteristics (e.g. friction) in different directions. The archetypal example of this is a file which cuts in the forward direction yet rubs in the backward direction. Directionality has been defined using a characteristic asperity model [2], but this just provides two-dimensional rather than three-dimensional directionality.

## 4 THREE-DIMENSIONAL SURFACE VECTORS

The technique described here takes an $x$–$y$–$z$ dataset of heights and transforms it into angular space which gives information on both the lay and directionality in terms of vectors as defined previously (Fig. 3). The technique involves two steps:

1. The application of an image processing mask to provide $x/y/$greyscale information which yields lay information. This analysis has been investigated in previous literature demonstrating the potential of using vectors for the visualization of surface lay [10].
2. The transformation of the greyscale to local gradient to give $x/y$ directionality information. At each point, a gradient vector is produced which, for convenience, can be considered to have two components. One is the lay direction of the surface plane, $\alpha$, and the other one is the gradient or directionality angle, $\beta$.

Values for $\alpha$ and $\beta$ are produced for each pixel within a greyscale image of the surface by using a gradient operator. Many gradient operators have been proposed for image processing. They are commonly used to provide local gradient information for edge tracing to identify a component outline. Numerous operators exist that use different mask sizes, shapes and weights [11]. Each operator generally consists of two masks (matrices) which are passed over the image sequentially, thus considering the vertical and horizontal areal surface components of the modelling vector. The Sobel operator is one of the most commonly used in image processing because it weights the gradient over a $3 \times 3$ area which gives a local average.

With respect to surface topography measurements, any differential operator could be used, depending upon the required resolution and sensitivity. However, the Sobel operator is used for two reasons:

1. It is a preferred one in image processing and is therefore well accepted [12].
2. It is a more stable operator as it averages local maxima with Gaussian weighting.

This means that the nearest neighbouring points in the image adjacent to the pixel being analysed are weighted according to their distance from it. Hence, the greater the distance between the analysis point and a neighbouring point, the less effect they have upon one another (T. A. Mitchell, Department of Manufacturing and Engineering Systems, Brunel University, 1997, personal communication). As the normal Sobel operator consists of a $3 \times 3$ operator matrix, this limits the resolution of the operator to a distance represented by nine adjacent data points within the three-dimensional Talysurf data file. The resolution of the technique described here depends directly on the digitization or spacing of the Form Talysurf instrument which can be defined by the user. This relationship is discussed in further literature by the authors [13].

## 5 CALCULATION OF $\alpha$ AND $\beta$ ANGLES

The $x$–$y$–$z$ data are stored as a two-dimensional array to which the operator masks, as previously detailed, are applied. Sobel's differential operator calculates the required values for each data point by considering the horizontal and vertical gradient functions $g_1$ and $g_2$ [14]:

$$g_1(x, y) = \mathrm{F}(x, y) \circledast h_1(x, y)$$

$$g_2(x, y) = \mathrm{F}(x, y) \circledast h_2(x, y)$$

where ✪ is the spatial convolution and $h_1$ and $h_2$ are $3 \times 3$ masks. The gradient $G$ and direction $\alpha$ are determined for every data point $(x, y)$ by trigonometrical analysis:

$$G_{(x,y)} = \sqrt{G_x^2 + G_y^2}$$
$$\alpha(x, y) = \tan^{-1}\left[\frac{g_2(x, y)}{g_1(x, y)}\right] \tag{1}$$

where $G_x = g_1(x, y)$ and $G_y = g_2(x, y)$.

In determination of angle $\beta$, $G_y$ and $G_x$ are the gradients in the $y$ and $x$ directions respectively. Fitting a plane through the point with these gradients gives

$$z = G_x X + G_y Y \tag{2}$$

The equation of a plane in its general form is given as

$$l_x + m_y + n_z = d = 0 \tag{3}$$

Therefore, equating (2) and (3) above gives

$$l = \frac{G_x}{t}, \qquad m = \frac{G_y}{t}, \qquad n = \frac{-1}{t} \tag{4}$$

where $t = \sqrt{G_x^2 + G_y^2 + 1}$. Rotating the plane anticlockwise in the $x/y$ plane (i.e. around the $z$ axis) in order that the steepest direction is in the $y$ axis yields

$$x = X\cos\theta + Y\sin\theta$$
$$y = -X\sin\theta + Y\cos\theta \tag{5}$$

Substituting equation (5) into (3) gives

$$l_X\cos\theta + l_Y\sin\theta - m_X\sin\theta + m_Y\cos\theta + n_z = 0 \tag{6}$$

Furthermore, the steepest gradient in $Y$ when the coefficient of $X$ is zero (no vertical gain) is

$$l\cos\theta - m\sin\theta = 0 \equiv \tan\theta = \frac{l}{m} = \frac{G_x}{G_y} = \frac{1}{\tan\theta} \tag{7}$$

and therefore

$$\sin\theta = \frac{l}{\sqrt{l^2 + m^2}}, \qquad \cos\theta = \frac{m}{\sqrt{l^2 + m^2}} \tag{8}$$

Substituting (8) into (3) gives

$$\sqrt{l^2 + m^2}y + nz = 0 \tag{9}$$

where $(\sqrt{l^2 + m^2}, n)$ is the cosine direction. Considering the present unit plane, along the $x$ axis

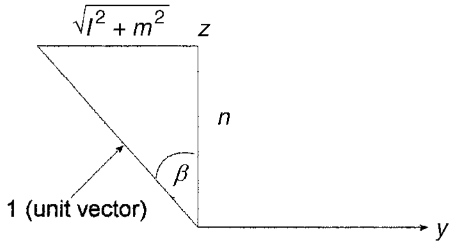


where

$$n \equiv \cos\beta$$
$$\sqrt{l^2 + m^2} \equiv -\sin\beta$$
$$\tan\beta = -\frac{\sqrt{l^2 + m^2}}{n} \tag{10}$$

Substituting the coefficients from the general formula in (4) gives

$$\tan\beta = \pm\sqrt{\frac{G_x^2/t^2 + G_y^2/t^2}{\pm 1/t}} \tag{11}$$

Therefore,

$$\tan\beta = \sqrt{G_x^2 + G_y^2}$$

the value for angle $\beta$ (gradient in terms of an angle orthogonal to the $\alpha$ direction) being given by calculating the arctan value of the gradient value as calculated via the Sobel operator.

## 6 VECTOR MAPS FOR SURFACES WITH ASYMMETRIC DIRECTIONALITY

The surfaces considered within this work, up to this point, are those that are symmetrical or periodic in an orthogonal direction to the predominant lay. However, for some engineering surfaces, the shape of the surface in the two directions perpendicular to the lay can have a pronounced effect on the performance of the surface *in situ*. This surface property is termed directionality within this work, as detailed previously (Fig. 3). A good example of this phenomenon is the cutting action of a hacksaw. The blade has a sawtooth cut that is asymmetric, and therefore, when the hacksaw blade is pulled backwards, there is low friction and some abrasion and, when the blade is pushed forwards, there is cutting. The asymmetry of the surface morphology in this case directly affects the functional performance.

Analysis of asymmetric surfaces using the $\alpha$–$\beta$ characterization technique was as follows. Asymmetric, turned surfaces were produced with a 90° included angle tool that was rotated 0, 15 and 30°, producing samples with a trail edge angle of 45, 30 and 15° respectively (Fig. 4). The pitch, feed rate, lubrication and spindle speed were kept constant for each case, and each turned specimen was turned in such a way as to produce relatively sharp included angles. A 5 mm × 5 mm area was analysed using the Form Talysurf series, with a diamond stylus of 2 μm tip radius. As the pitch is constant for all specimens, the resulting images are comparable for each asymmetry. The tools used were sharp and the workpiece material was free machining steel. In the three greyscale,

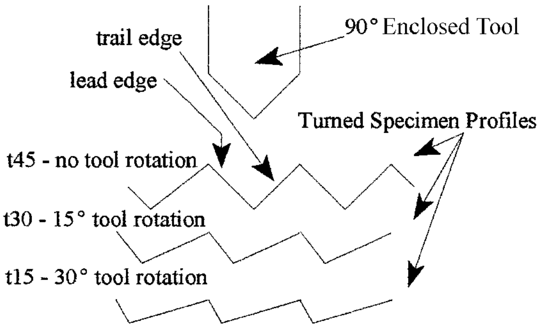


**Fig. 4** Schematic diagram of turned specimen asymmetric surfaces

raster scan images, the surfaces appear to be regular with few discontinuities (Figs 5 to 7). However, the corresponding histograms show two distributions around the ideal impulses. This is because the traces were from real surfaces with localized discontinuities and perturbations caused by laps, folds, tears, microcracks and vibrations which cannot be identified visually from the raster scan images. With an increase in tool rotation, the angle of the lead and trail edges of the resulting turned profile increases and decreases respectively, as shown in Table 2.

For each of these specimens, the histograms (Figs 5 to 7) show two peaks which represent the lead and trail edge surfaces. The histograms detect the change in the lead

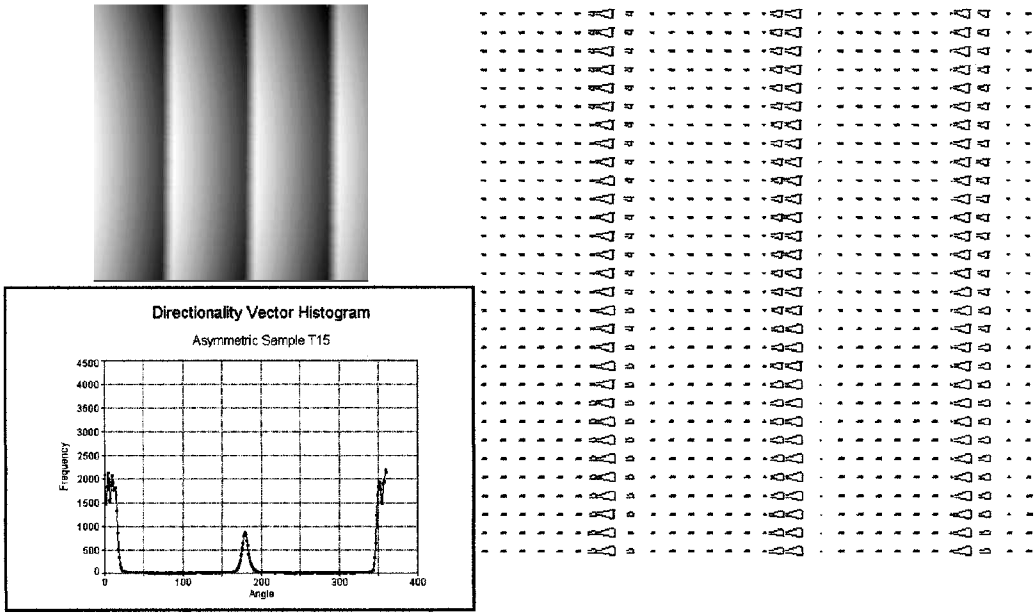


**Fig. 5** Asymmetric surface t15 (30° tool rotation)

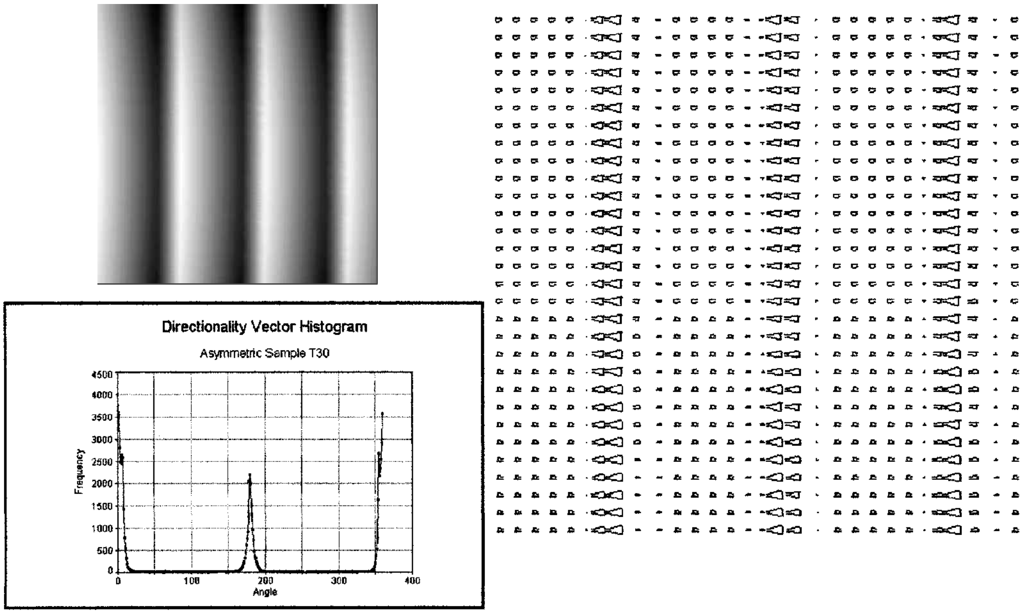


**Fig. 6** Asymmetric surface t30 (15° tool rotation)

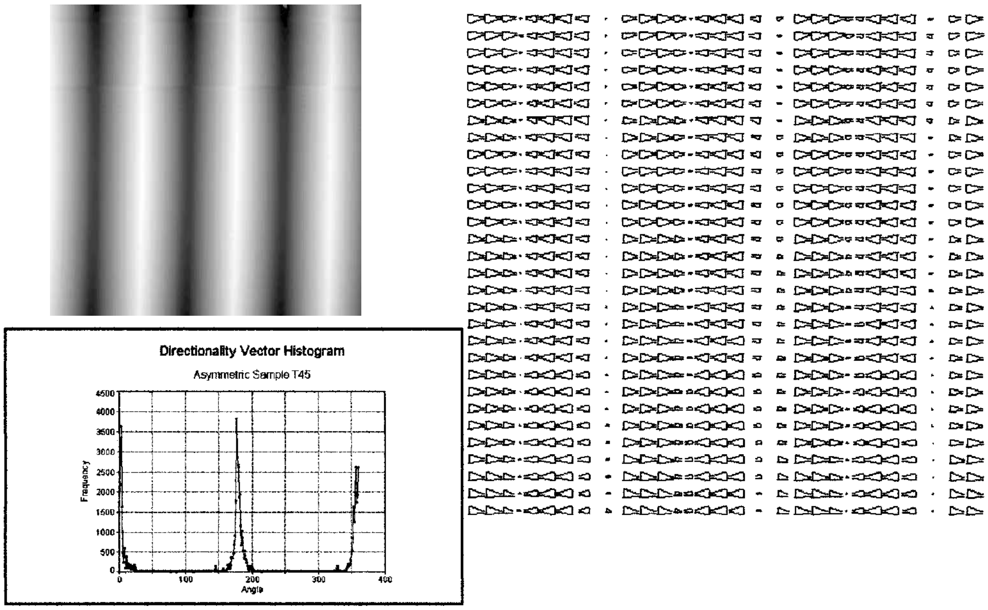


**Fig. 7** Asymmetric surface t45 (no tool rotation)

and trail edge surface angles, which results in a change in the heights of the peaks corresponding to the area of these surfaces.

As the feed rate and the depth were kept constant for the asymmetric samples, the depth of cut of the profile therefore varies, which results in a change in the actual surface area of the lead and trail edge surfaces. Analysis of the magnitude distribution of the modelling vectors corresponded to this change.

Conventional three-dimensional techniques are unable to describe the asymmetry (directionality) of the samples analysed above and as defined in Fig. 3. Analysis of the specimen surfaces renders the three-dimensional lay angle $\alpha$ and directionality $\beta$ versus frequency graphs (Fig. 8) for the asymmetric specimens t15, t30 and t45. These graphs detect the change in the three-dimensional lead and trail edge angles, as well as characterizing the asymmetry of the specimens. Again, if the asymmetric specimens produced were without noise, the peaks of the three-dimensional graphs discussed above would be impulses representing the lead and trail edge angles. However, as the turning process employed is not ideal, there is some spreading of the resulting data. These results cannot be completed using conventional three-dimensional parameters as the surface properties investigated are three-dimensional and dependent on the directionality of the surface. Previous work relating wear to the asymmetry of turned samples [**15**, **16**] has only been able to use conventional two-dimensional parameters to specify surface texture. Hence, this new characterization technique may prove a useful aid to the wear analysis of asymmetric samples.

**Table 2** Asymmetric specimen lead and trail edge angles

| Specimen | Tool rotation (deg) | Lead edge angle (deg) | Trail edge angle (deg) |
|---|---|---|---|
| t15 | 30 | 75 | 15 |
| t30 | 15 | 60 | 30 |
| t45 | 0 | 45 | 45 |

## 7 CONCLUDING COMMENTS

The properties and interactions of engineering components *in situ* are observed to be three-dimensional quantities. Hence, the surface topography and texture of engineering components directly affect both function and component lifetime. A requirement therefore exists for the measurement and characterization of engineering surfaces to be a three-dimensional technology. Present metrological standards include single-trace two-dimensional surface parameters, the most commonly used being $R_a$ (average roughness deviation from the mean surface). These parameters are shown to be inadequate to define particular three-dimensional surface properties. However, at present there are no three-dimensional metrological standards. Proposals for three-dimensional parameters have not been accepted by the International Standards Organization (ISO). A new technique of surface texture representation is proposed within this work, utilizing vector modelling. The technique is tested on theoretical and industrial surfaces and distinguishes between each one in terms of three-dimensional lay and directionality. The technique permits quantitative measurement of the asymmetry of surface finishes and detection of changes in three-dimensional surface

 

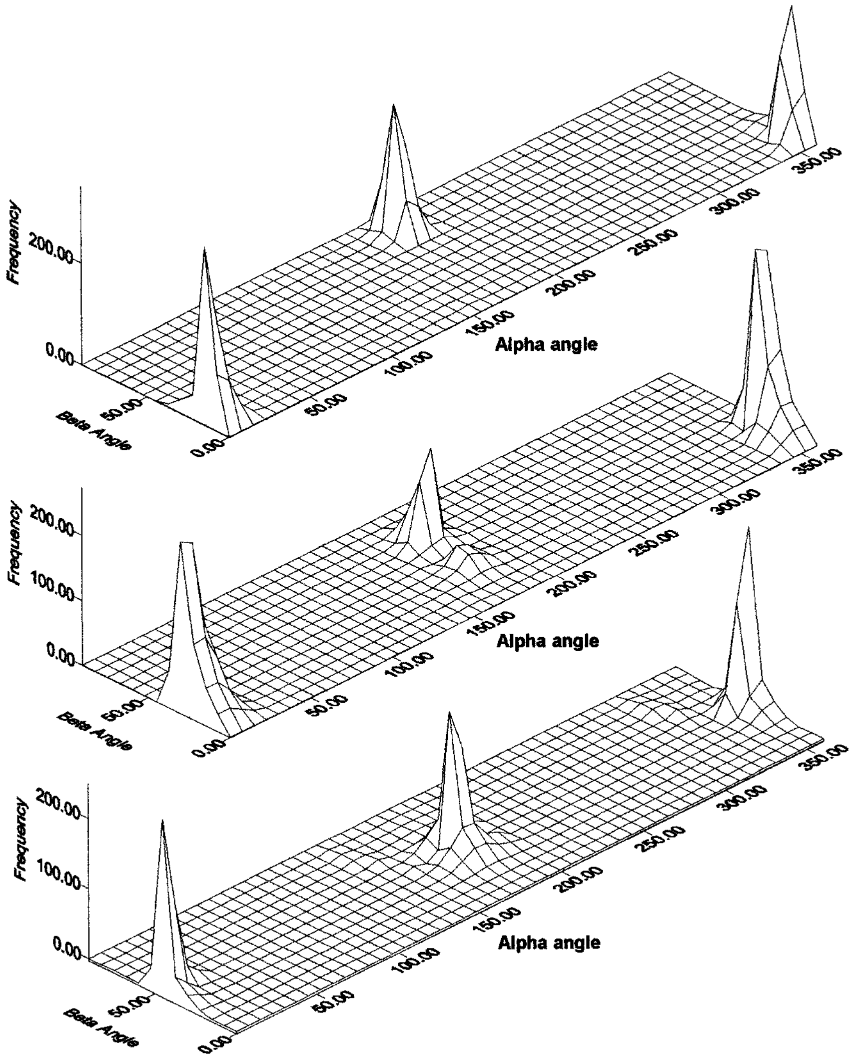


**Fig. 8** Graphs of lay angle $\alpha$ and directionality $\beta$ against frequency: (a) for surface t15, (b) for surface t30 and (c) for surface t45

properties which existing techniques cannot detect. Previous work by the authors has shown that vector modelling also facilitates detection and levelling of surfaces, improved visualization, user-defined filtering and areal representation of three-dimensional properties [**11**]. This technique allows the analysis of three-dimensional surface topography in a new and novel way which is designed to assist engineers in their assessment of engineering surfaces.

Future investigation of the effect of digitization and operator matrix size, proposed by this technique, may provide further mathematical tools to describe engineering surface texture.

## ACKNOWLEDGEMENTS

This work was undertaken as a result of an EPSRC-funded case award, sponsored by Taylor Hobson Limited. This research was completed while Dr J. M. Burrows was a research engineer at the Department of Manufacturing and Engineering Systems at Brunel University. The authors also wish to thank Dr T. A. Mitchell and Dr R. Bowden for their advice concerning image processing.

## REFERENCES

1 **Tonshoff, H. K.** and **Brinksmeier, E.** Determination of the mechanical and thermal influences on machined surfaces by micro hardness and residual stress analysis. *Ann. CIRP*, 1980, **29**(2), 519–530.
2 **Griffiths, B. J., Dong, G.** and **Gawne, D. T.** A definition of the topography of grit blasted surfaces for plasma sprayed alumina coatings. *Trans. ASME, J. Mfg Sci. Engng*, November 1998, **120**, 230–237.
3 *Surface Texture Parameters*, Publication 800-303/496 5MCP, 1996 (Taylor Hobson Limited).

4 **Burrows, J. M.** and **Griffiths, B. J.** The effect of 3-dimensional surface finish upon component wear and product life cycle. *Advances in Mfg Technol.*, 1996, **10**, 231–235.

5 **Furze, D. C., Griffiths, B. J., Walton, S.** and **Franks, A.** A short duration strip drawing rig. *Int. J. Mach. Tools Mf.*, 1992, **32**(5), 757–766.

6 **Dong, W. P., Mainsah, E., Stout, K. J.** and **Sullivan, P. J.** Three-dimensional surface topography—review of present and current trends. *Three-Dimensional Surface Topography; Measurement, Interpretation and Applications*, 1994, pp. 65–88 (Penton Press).

7 **Stout, K. J., Sullivan, P. J., Dong, W. P., Mainsah, E., Luo, N., Matia, T.** and **Zahouani, H.** The development of methods for the characterisation of roughness in three dimensions. European Commission Report EUR 15178EN, 1993.

8 **Barre, F., Lopez, J.** and **Mathia, T. G.** New methods for characterising the anisotropy of engineering surfaces. In Proceedings of 7th International Conference on *Metrology and Property of Engineering Surfaces*, Chalmers University, Sweden, 1997, pp. 479–486.

9 **Thomas, T. R.** 3-D structure function applied to engineering surfaces. In Proceedings of Conference on *Engineering Surfaces*, Corps de La Salette, 3–4 June 1998.

10 **Burrows, J. M.** and **Griffiths, B. J.** A vector modelling technique for the representation of 3-dimensional surface topography. *Int. J. Mach. Tools Mf.*, 1998, **38**(5–6), 537–542.

11 **Gonzalez, R. C.** and **Woods, R. E.** *Digital Image Processing*, 1994 (Addison-Wesley).

12 **Burrows, J. M.** Three-dimensional vector modelling of engineering surface topography. PhD thesis, Brunel University, 1999.

13 **Gomez, S., Hale, K., Burrows, J. M.** and **Griffiths, B. J.** Measurement of surface defects on optical components. *Measmt Sci. Technol.*, 1998, **9**, 607–616.

14 **Sobel, I.** Camera models and machine perception AIM-21. Stanford Artificial Intelligence Laboratory, Palo Alto, 1970.

15 **Allen, A. F.** and **Brewer, R. C.** The influence of machine tool variability and of tool flank wear on surface texture. In Proceedings of 6th International MTDR Conference, 1965, pp. 301–314.

16 **Jahanmir, S.** and **Suh, N. P.** Surface topography and integrity effects on sliding wear. *Wear*, 1977, **44**, 87–99.

 